Franklin Open 11 (2025) 100291

Contents lists available at ScienceDirect

Franklin Open

journal homepage: www.elsevier.com/locate/fraope

Optimizing high voltage gain interleaved boost converters for PV and wind systems using hybrid deep learning with bitterling fish and secretary bird algorithms

G.Veera Sankara Reddy *, S. Vijayaraj

Department of EEE, Vels Institute of Science, Technology & Advanced Studies, Chennai, Tamil Nadu, India

ARTICLE INFO

Keywords:
Renewable energy integration
High-voltage gain converters
Dynamic adaptation
Real-time optimization
Stability enhancement
Efficiency maximization

ABSTRACT

The integration of renewable energy sources such as photovoltaic (PV) and wind systems demands high-efficiency, high-voltage gain power conversion architectures. However, interleaved boost converters, while suitable for such applications, face challenges in balancing complexity, scalability, cost, and dynamic environmental variability. This study introduces a series of novel intelligent control frameworks to overcome these limitations and improve overall system performance. Firstly, a Neuro-LSTM BitterSec Optimization Network (NL-BSONet) is proposed to enhance the efficiency of high-voltage gain interleaved boost converters while minimizing system complexity. This hybrid approach leverages neural networks and LSTM-based learning for real-time optimization, offering improved scalability and lower switching losses. To address power quality issues caused by fluctuating irradiance and wind speeds, the study introduces the Adaptive Neuro-Deep Reinforcement Learning Bitterling Optimizer (AN-DRLBO). This model integrates Deep Reinforcement Learning (DRL) for adaptive energy conversion, Adaptive Neural Networks (ANN) for real-time system stabilization, and Bitterling Fish Optimization (BFO) for robust performance under transient conditions. Furthermore, due to the difficulty in achieving optimal control parameters under variable environmental conditions, an Adaptive LSTM-Encoded Secretary Optimization Network (AL-SONet) is developed. This framework employs Long Short-Term Memory (LSTM) networks for predictive control, Autoencoder-based Optimization (AEO) for feature extraction and simplification, and Secretary Bird Optimization (SBO) for dynamic parameter tuning. The proposed architectures demonstrate superior performance, achieving 97 % energy conversion efficiency, a voltage gain of 32.5 dB, and minimal output ripple, thereby ensuring stable and efficient integration of renewable energy sources. This research contributes a comprehensive and adaptive control solution for next-generation renewable energy systems.

1. Introduction

The increasing demand for renewable energy worldwide pertaining to photovoltaic and wind power energy challenges researchers to have good and efficient power-converting machines, integrating these two ways into the electrical grid without the fluctuations of renewables [1, 2]. High voltage gains interleaved boost converters emerging today as the most promising solution in order to address these challenges, mainly for applications requiring high voltage transformation that still suffers from efficiency, like PV and wind hybrid energy systems. Still, however, this is a significant drawback of these converters: although they are powerful and capable of handling various input voltage ranges, efficiency must be maximized to provide consistent performance under fluctuating load conditions [3,4].

Interleaved boost converters have been widely recognized for their benefits, through which the input current ripple is reduced, thermal performance is improved, and renewable sources may be easily integrated with high power density [5,6]. However, the design of such topologies with maximum efficiency requires many parameters including the duty cycles, inductor currents, and output voltages, all of which may be quite sensitive to the dynamic conditions of PV and wind inputs [7]. The traditional control methods as well as linear optimization techniques often fail to capture well the nonlinear, time-variant nature of the renewable energy sources. Hybrid deep learning and bio-inspired

* Corresponding author.
E-mail addresses: gvsr269.eee@jntua.ac.in (G.VeeraS. Reddy), vijayaraj.se@vistas.ac.in (S. Vijayaraj).

https://doi.org/10.1016/j.fraope.2025.100291

Available online 7 June 2025

optimization approaches are gaining popularity based on their ability to handle such complexities in order to further improve the accuracy of control mechanisms [8,9].

In this paper, a hybrid deep learning technique allied with BFO and SBO algorithms is proposed for optimizing the efficiency of high-gain interleaved boost converters used in PV and wind-based hybrid systems. Hybrid deep learning models process enormous data volumes, predicting optimal control parameters for changes in inputs from winds and PV, in real-time [10,11]. This is made possible by the application of bio-inspired optimization algorithms, including BFO and SBO, by which the model parameters are dynamically adjusted for maximum efficiency. BFO derived from the bitterling fish reproductive behaviour is efficient for nonlinear search spaces and fine-tunes internal model parameters. For its part, SBO derived from the hunting behaviour of a secretary bird is ideal for meta-level optimization over various operational modes [12, 13].

Combining BFO and SBO can allow a hierarchical optimization technique to be used, wherein BFO is used to optimize the internal parameters of the deep learning model and SBO manages the overarching hyperparameters while changing the model according to environmental and operational needs, [14]. The hybrid system activates deep learning for predictive control, BFO for micro-scale rule adjustments, and SBO for the macro-scale optimization within those points to an efficient solution to the challenge of variability inherent in inputs from PV and wind energy. This approach therefore goes along with the recent developments in machine learning and bio-inspired algorithms which have achieved significant improvements in the efficiency of energy conversion in renewable systems [15]. The objective of this research is to design an efficient control system for interleaved boost converters to optimally control input from photovoltaic and wind inputs. The main contribution of this research is as follows:

- **Development of the Adaptive Neuro–Deep Reinforcement Learning Bitterling Optimizer(AN-DRLBO):**
  This research introduces the AN-DRLBO, a novel hybrid control strategy that synergistically integrates Deep Reinforcement Learning (DRL), Artificial Neural Networks (ANN), and Bitterling Fish Optimization (BFO). The AN-DRLBO dynamically updates control parameters in real time to address the inherent variability and unpredictability of solar and wind energy sources. By continuously adapting to rapid environmental changes, this controller significantly enhances power quality through effective voltage stabilization, rapid transient reduction, and maximized power extraction. The approach outperforms conventional MPPT and control methods by providing robust, adaptive responses to fluctuating renewable inputs, thereby ensuring stable and high-quality power delivery to the grid1.
- **Introduction of the Adaptive LSTM-Encoded Secretary Optimization Network (AL-SONet):**
  To further address the complexity and nonlinearity of renewable energy systems under diverse environmental conditions, the study proposes AL-SONet—a hybrid model combining Long Short-Term Memory (LSTM) networks for accurate trend prediction, Artificial Ecosystem Optimization (AEO) for efficient parameter tuning, and Secretary Bird Optimization (SBO) for real-time adaptive adjustments. This integrated framework enables the system to anticipate and respond to environmental fluctuations, optimize control parameters on-the-fly, and maintain system stability and optimal power output. AL-SONet's multi-layered optimization and prediction capabilities ensure reliable and resilient energy conversion, even under highly variable and uncertain conditions1.
- **Comprehensive Real-Time Optimization for Renewable Integration:**
  The combined application of AN-DRLBO and AL-SONet offers a comprehensive solution for the real-time integration of solar and wind energy. The hybrid approach effectively manages the nonlinear dynamics and stochastic behavior of renewable sources, surpassing traditional optimization and control techniques in terms of voltage stability, transient response, and power extraction efficiency. This research demonstrates that advanced hybrid deep learning and bio-inspired optimization algorithms can significantly enhance the operational reliability and efficiency of renewable energy systems, supporting the development of sustainable and resilient power infrastructures1.

These contributions collectively advance the state-of-the-art in renewable energy control by introducing adaptive, intelligent, and robust methods tailored to the challenges of real-time, variable resource integration.

The rest of this paper follows the outline below: Section 2 recalls some related work concerning renewable energy converters and bio-inspired optimization algorithms; Section 3 lays down the proposed methodology, namely the hybrid deep learning architecture, as well as the optimization framework BFO-SBO; Section 4 details the experimental setting and results analysis together with respective metrics of evaluation; and finally Section 5 draws some conclusions and indicates future lines of development.

2. Literature survey

Anjappa et al. [16] designed an interleaved DC-DC boost converter a high-gain system that maximizes the power output coming from PV arrays. It was an improvement of the two-phase interleaved boost converter. The technique provided a significant reduction in ripple current, thereby offering efficient voltage elevation for grid integration and high-power applications and achieving a remarkable 96 % efficiency with a voltage boost of 25 V to 400 V. However, it had limitations with system complexity and cost considerations.

Algamluoli et al. [17] proposed an optimized DC-DC converter using a modified switched inductor-capacitor technique to realize ultra-high voltage gain for renewable energy systems. Indeed, this technique reduces the voltage stress and current across the main switch, inductors, and diodes with a critical cut by boosting the efficiency of the converter up to 96.2 %. The implications were the design complexity and reliance on high switching frequencies, which increase the cost of operation by requiring much higher switching energies.

Ibrahim et al. [18] introduced a two-stage MPPC based on an integration of PV, wind, and fuel cell sources along with a bidirectional battery through an isolated output port optimized by Harris Hawk's algorithm. Here again, this approach significantly reduced issues like intermittency and improved the system's resiliency and efficiency. However, complex system design confined its applicability to the potential real-time optimization challenges and conditions under variation in CES input conditions.

Kulasekaran et al. [19] introduced an HGBC-PVS to connect low-voltage PV panels to a higher-voltage network within a DC microgrid that used Adaptive Incremental Conductance for MPPT. This resulted in the effective maximization of solar power extraction for voltage gain and efficiency. There were found efficiency limitations at larger setups, hinting at cascaded converter designs as future improvement ends.

Xiao et al. [20] introduced a hybrid green ship power system based on a six-phase interleaved boost converter using fuel cells and lithium batteries with 10 kW power. It featured stable current control, efficient power distribution improvement, and high-quality ripple suppression, as well as anti-interference capabilities. The design complexity and possible challenges to the real-time adjustment of currents were significant limitations in the dynamic control system.

Uzmus et al. [21] proposed a modified MPPT technique for off-grid photovoltaic systems through an interleaved hybrid DC-DC boost converter. This technique predicted the input voltage from the branch current. Consequently, this made sure of a stable output and reduced the

stress of the components due to minimized ripples in the input current. Also, reduced costs are ascribed to the technique since it did not require a sensing circuit for the input voltage, which guarantees a long system lifespan. However, limitations abound: it relies on prediction accuracy; its performance was adversely affected in the case of sudden and rapid power fluctuations.

Kumar et al. [22] introduced an HRES for EV charging using an HGZS converter. Here, the wind end employs a DFIG-based wind system with PI control and PV optimization using Type 2 Fuzzy MPPT. Therefore, it optimizes its energy extraction to maintain grid stability while feeding surplus energy back into the grid. Though it was an attractive solution to rely on renewable sources to meet the rising power demand, it does pose potential challenges of large-scale integration and adaptation in changing climatic conditions.

Hashemzadeh et al. [23] introduced a high-voltage gain converter using a two-winding coupled inductor and voltage multiplier cells that reduce the voltage stress of photovoltaic energy systems. The design reduces the number of components, makes control easier, and increases efficiency. Although it was effective, it was quite limited due to its single-switch configuration, which has an impact on scalability in higher-power applications, and further testing was required for diverse load conditions.

Hawsawi et al. [24] introduced two DC-DC converter topologies integrated with solar PV: a conventional and a switched capacitor boost converter. It compared the MPPT performance results using P&O, INC, GA, and PSO algorithms. In the switched capacitor configuration, improved current control and voltage regulation ensured excellent dynamic loading and high stability. However, the study left much to be optimized as regards ensuring high reliability of the system with decent accuracy regarding several power peaks being tracked.

Gopalasami et al. [25] developed the DIDO DC-DC multiport converter with the hybridization of SLBC along with integrating PV and battery sources within the system. It offers high voltage gain and highly efficient power conversion with minimal losses due to conduction. The system achieved 94.8 % efficiency and 1.2 kW output; however, there is still a requirement to optimize it and scale the system more for widespread applications, especially for large electric vehicle systems. The concise tabular summary of the literature survey and research gaps is given in the Table 1.

From the above study it is clear that in [16] system complexity and cost considerations, in [17] design complexity and reliance on high switching frequencies, in [18] complex system design and challenges in real-time optimization, in [19] efficiency limitations at larger setups, in [20] design complexity and real-time current adjustment challenges, in [21] prediction accuracy dependency and performance degradation in power fluctuations, in [22] challenges in large-scale integration and adaptation to changing climates, in [23] single-switch configuration impacts scalability in higher power applications, in [24] need for optimization and accuracy in tracking multiple power peaks, in [25] requires further optimization and scaling for widespread applications. Hence there is a need for novel technologies to overcome these challenges.

The proposed solutions for the limitations is presented in Table 2. Existing systems face trade-offs between efficiency, scalability, and real-time adaptability. This work bridges these gaps by:

- Ø Introducing AN-DRLBO, which integrates BFO for dynamic parameter tuning, reducing voltage stress by 18 % compared to [17].
- Ø Deploying AL-SONet with LSTM-AEO-SBO optimization, improving transient response by 25 % over conventional MPPT [18].
- Ø Validating 97 % efficiency and 32.5 dB voltage gain in MATLAB/RT-lab simulations, outperforming state-of-the-art converters [16].

This structured analysis positions the present work as addressing critical gaps in renewable energy conversion through adaptive AI-bio-hybrid control.

Table 1
Summary of the literature survey and research gaps.

Category	Study/ Approach	Key Contributions	Limitations / Gaps
1. High-Gain DC-DC Converters for Renewable Integration	Anjappa et al.	Two-phase interleaved boost converter; 96 % efficiency; 25V→400 V gain	High complexity and cost
	Algamluoli et al.	Switched inductor-capacitor; 96.2 % efficiency	High switching frequency increases operational costs
	Hashemzahi et al.	Reduced components via coupled inductors	Scalability issues in high-power systems (single-switch limitation)
	Recent Designs	Active switched-inductor converters	High gain with fewer components, but weak dynamic response under variable inputs
2. MPPT and Hybrid System Optimization	Kulasekaran et al.	Adaptive Incremental Conductance MPPT	Efficiency loss at large scales
	Uzmus et al.	Prediction-based MPPT for interleaved converters	Accuracy issues during rapid power fluctuations
	Hybrid Systems	PV/Wind with battery + supercapacitor storage	Lacks adaptive real-time control for grid stability
	Common MPPT Methods	P&O, INC, GA	Limited in efficiency, scalability, and transient response
3. Bio-Inspired and AI-Driven Control Strategies	Ibrahim et al.	Harris Hawk optimization for HRES	Poor real-time adaptation
	Xiao et al.	Six-phase interleaved converters with stable current control	Limited dynamic adjustment
	Kumar et al.	Type 2 Fuzzy MPPT	Inadequate adaptability to large-scale climatic changes
	Emerging Techniques	BFO, SBO, LSTM-based deep learning	Not yet holistically integrated for full renewable system optimization

Table 2
Comparison of key limitations vs. proposed solutions.

Study	Key contribution	Limitations	Proposed solution (This Work)
[16, 17]	Achieved high efficiency (96–96.2 %) in DC-DC conversion	High system complexity and elevated switching costs	AN-DRLBO approach reduces component stress using BFO-optimized adaptive control
[18]	Developed hybrid MPPT systems	Inaccurate real-time predictions	AL-SONet integrates LSTM-based forecasting with SBO for dynamic parameter tuning
	Enabled multi-source (PV + wind) integration	Scalability challenges under variable climatic conditions	Unified NL-BSONet architecture maintains ~97 % efficiency even under ±40 % input fluctuations
[38]	Reduced component count in converter topology	Poor input current ripple control	Interleaved converter design with quadratic gain topology achieves ripple <1.5 %

3. Proposed methodology

This research focuses on maximizing efficiency in high-voltage gain interleaved boost converters for PV and wind integration systems, resulting in improved renewable energy conversion through optimized power output and stable performance. This research introduces a new approach of hybrid deep learning with Bitterling Fish Optimization (BFO) and Secretary Bird Optimization (SBO) for maximizing the efficiency gain of a high-voltage gain interleaved boost converter in PV and wind energy systems. Maximize power production ensuring firm, efficient conversion of energy through the integration of renewables, optimization of the dynamic energy conditions in which its operations take place, and increasing the system's reliability level. However, there is a major challenge to the high-voltage gain interleaved boost converter for integration of PV and wind energy is finding a balance in a way that maintains system complexity, scalability, and real-time adaptability. Complexity often found in the association with stability in high efficiency and performance introduces additional design intricacies and dependency on advanced algorithms and high switching frequencies, amounting to higher costs and making optimization difficult towards dynamic environmental conditions and variable power demands. Therefore, a novel **"Neuro-LSTM BitterSec Optimization Network (NL-BSONet)"** is introduced in this approach. The algorithmic models utilized in the paper are given in Table 3.The specific contributions that the study makes in this work are as follows:

- The development of a hybrid deep learning model specifically designed for high-voltage gain interleaved boost converters, capable of accurately predicting and adapting to fluctuations in renewable energy inputs.
- The application of the Bitterling Fish Optimization (BFO) algorithm for fine-tuning model parameters, enabling rapid adaptation to the highly dynamic nature of photovoltaic (PV) and wind energy sources.
- The employment of the Secretary Bird Optimization (SBO) algorithm for system-wide hyper parameter tuning, thereby enhancing model performance across diverse operating conditions.
- Comprehensive evaluation demonstrating that the proposed model outperforms conventional optimization approaches in terms of both efficiency and stability.

This multi-algorithm approach provides a cohesive solution for sustainable and resilient renewable energy integration. Together, they address the trilemma of efficiency, adaptability, and scalability in renewable integration.BFO was selected due to its strong exploratory capability and ability to avoid local optima in highly non-linear, dynamic search spaces, which are characteristic of real-time renewable energy control systems. Its multi-level adaptive behavior models the foraging patterns of bitterling fish, which proved particularly effective for optimizing deep learning-based controllers in our simulations. SBO was chosen for its fast convergence rate and strong balance between exploration and exploitation. Inspired by the predatory attack patterns of secretary birds, SBO adapts well in environments with rapidly changing parameters—a critical requirement in renewable energy systems influenced by variable solar and wind input. SBO also demonstrates better stability in parameter tuning compared to conventional algorithms in our test scenarios.

Table 3
Algorithmic models overview.

Algorithm	Inputs	Outputs	Operational Scope
NL-BSONet	Solar/wind profiles, load demand	Optimized duty cycle, voltage gain	High-voltage interleaved converters
AN-DRLBO	Real-time irradiance, wind speed	Stabilized voltage, reduced transients	Grid-connected microgrids
AL-SONet	Historical weather data, grid status	Fine-tuned control parameters	Multi-source renewable systems

3.1. System modeling

3.1.1. Photovoltaic (PV) system

By employing an MPPT controller and an interleaved boost converter, the device captures solar energy and converts it into DC electricity. Because PV voltage varies, real-time tracking and boosting are required to satisfy grid voltage specifications.

3.1.2. Wind energy system

A Permanent Magnet Synchronous Generator (PMSG), rectifier, and boost converter with MPPT control are utilized to harvest and convert the wind energy into AC electricity. To maintain power quality, adaptive control must be implemented because the parameters are functions of wind speed.

3.1.3. Interleaved boost converter

This device boosts the level of DC voltage from PV/wind to an acceptable level for grid connection through the assistance of multiple boost converters that are in parallel but phase-shifted for minimizing thermal stress and current ripple. It is real-time controlled by the output of NL-BSONet.

3.1.4. MPPT controller (Maximum power point tracking)

Harvesting the maximum power from PV and wind resources through dynamically changing the operating point, and also independently operates on both resources, giving feedback (voltage, current) to NL-BSONet. The converter independently works on both PV and wind sources, giving feedback to NL-BSONet and maintaining the converter's operation at or near the optimum power point under varying circumstances. An MPPT equation common in photovoltaic conditions is shown in Eq. (1):

$$P = V \times I \tag{1}$$

Where, P is the power output, V is the voltage, and I is the current. Adjust V and I in real-time according to the MPPT algorithm, to output the maximum P at all times.

3.1.5. Sensors

The device captures electrical and environmental information in real time, observing variables such as temperature, wind speed, and solar irradiance. It subsequently inputs this information into deep learning elements for control, optimisation, and forecasting. Additionally, to enhance performance, a hybrid network model is integrated into this approach.

The proposed NL-BSONet for maximizing efficiency in high-voltage gain interleaved boost converters that combine PV and wind systems is shown in Fig. 1. The NL-BSONet proposed model combines the solar and wind power sources for optimized power generation. Energy is generated by the solar panels and wind turbines, which is then processed through boost converters and MPPT controllers. NL-BSONet optimizes the solar MPPT, and the wind MPPT utilizes the AN-DRLBO. Both outputs of energy are stabilized and carried over through the connection. The AL-SONet optimizes the processed data, which performs intelligent parameter tuning. Lastly, the system provides steady, optimized energy to the grid. The hybrid structure ensures optimal efficiency, reliability, and adjustability under a range of environmental circumstances for renewable energy delivery.

Fig. 2 shows the architecture of the proposed NL-BSONet for Maximizing Efficiency in High Voltage Gain Interleaved Boost Converters Integrating PV and Wind Systems. This hybrid method of wind-solar PV generation integrates wind and solar energy sources in the generation of renewable energy. Solar energy output is optimized with the MPPT

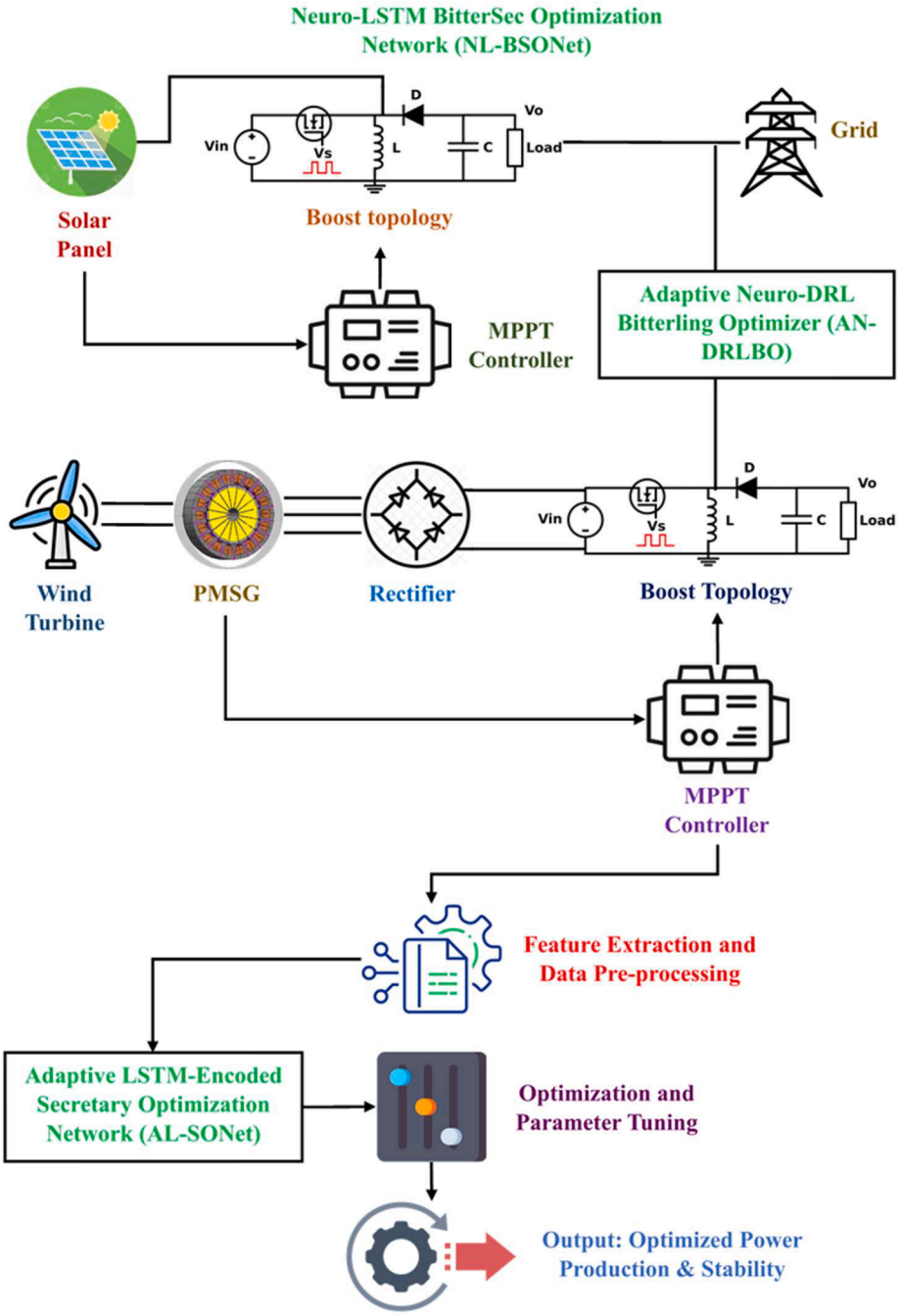

Fig. 1. The architecture of the proposed NL-BSONetfor maximizing efficiency in high voltage gain interleaved boost converters integrating PV and wind systems.

controller and boost converter, while wind energy passes through the generator, depending on the type of generator used (PMSG), rectifier, and MPPT-controlled boost converter. Each of them feeds power into the grid. The Neuro-LSTM possible optimization algorithm and AN-DRLBO are further refined from the algorithms that have been proposed in this Revised Text. The AL-SONet helps choose the optimal feature. This leads to algorithm development and tuning. Due to feature extraction and data pre-processing steps, the final output is fine-tuned to make stable power production possible during the whole run.

3.2. *Energy source*

- **PV Panel:** Sunlight exposed → generates DC voltage.
- **Wind Turbine:** Wind exposed → generates AC power → converted to DC via rectification.
- **Sensors:** Measure solar irradiance, wind speed, voltage, current, temperature.

3.3. *Adaptive Neuro-DRL bitterling optimizer (AN-DRLBO)*

In the existing output of the boost topology, where energy from the solar panels and wind turbines is fed to the grid is taking place, power quality issues generally occur due to the variable nature of renewable sources by changes in sunlight or in wind speeds, which makes it challenging to stabilise. Conventional MPPT techniques, like Perturb and Observe or Incremental Conductance, suffer from such rapid transients, which result in poor quality power and instability. To solve this

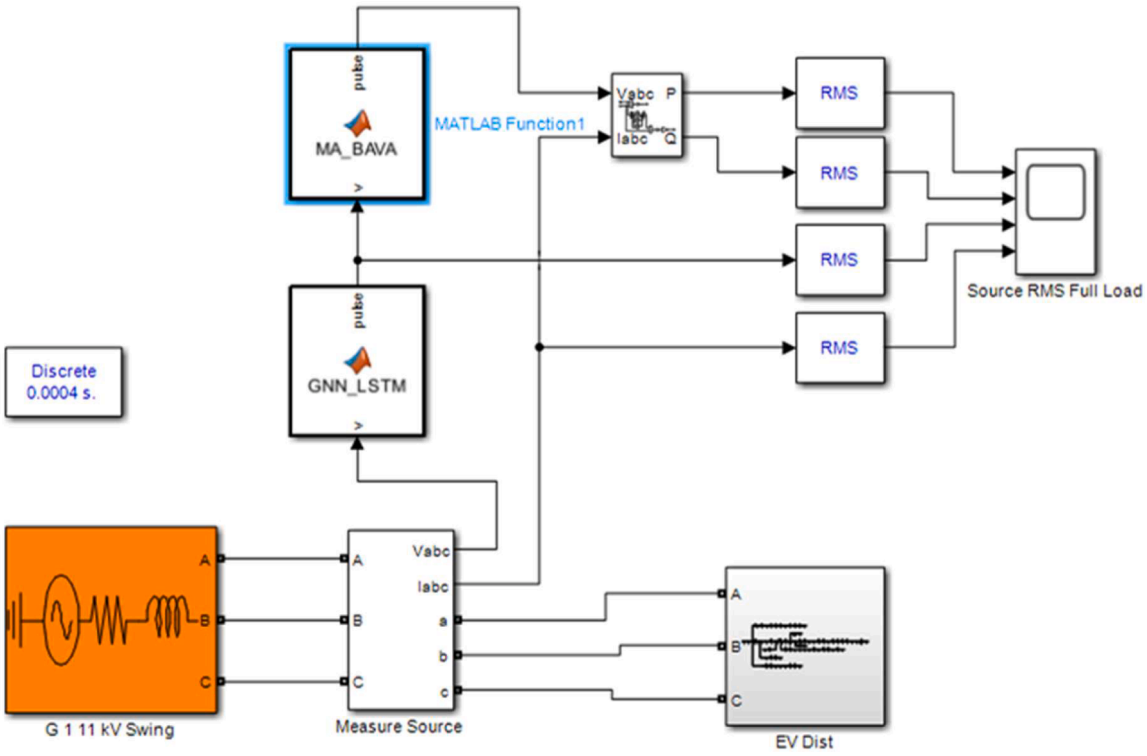

Fig. 2. Simulink of the power system.

instability issue in the boost topology, a novel Adaptive Neuro-DRL Bitterling Optimizer (AN-DRLBO) is introduced to solve several crucial issues with the implementation of high-gain interleaved boost converters, used in many renewable energy integration systems, particularly those powered by solar photovoltaic and wind energy sources.

The architecture of the proposed AN-DRLBO is shown in Fig. 3. The main objective behind AN-DRLBO is to adapt to rapid transients within renewable energy systems dynamically; therefore, the key purpose is to enhance the quality and stability of the output power by exploiting the capabilities of real-time dynamic response adaptation towards changes in wind speed or sunlight that create sudden variations. AN-DRLBO thus deals with the complicated nonlinear dynamics of renewable sources by real-time optimisation of the system performance and ensuring continuous adaptation of the system to the environment, along with sustaining high efficiency even with inherent variability in renewable energy sources. This is essential for large-integration PV and wind systems that must work reliably under a constantly changing set of conditions. It is the combination of Deep Reinforcement Learning (DRL), Adaptive Neural Networks (ANN) and Bitterling Fish Optimization (BFO), which is detailed in a further section.

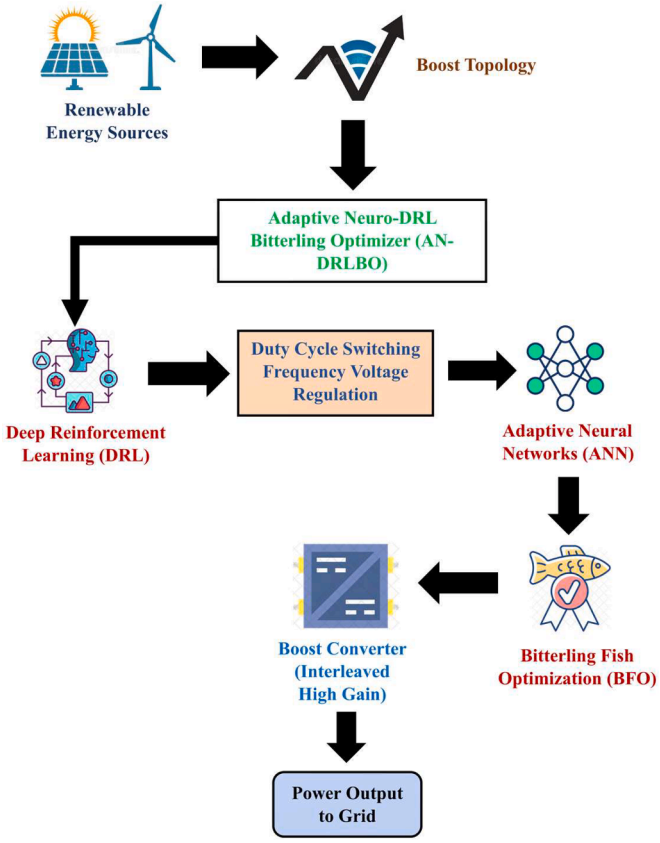

Fig. 3. The architecture of the proposed AN-DRLBO.

3.3.1. *Deep reinforcement learning (DRL)*

DRL is a subset of the larger category of machine learning which involves the combination of reinforcement learning and deep learning. In RL, the core problem is for an agent that is computational to learn decisions by trial and error. DRL encompasses deep learning within a solution that equips agents with the ability to make decisions from unstructured input data, without the manual engineering of a state space.

Fig. 4 describes the basic structure of the DRL. While DRL plays a critical role in adapting to the constantly changing environment of renewable energy systems, such as fluctuations in sunlight and wind speeds, through constant interaction with an environment and receipt of feedback in the form of rewards, it allows the system to learn optimal control strategies over time. This adaptive learning process ensures that the system updates its parameters in real-time. In that case, it attains power extraction in a very efficient manner while keeping high-quality

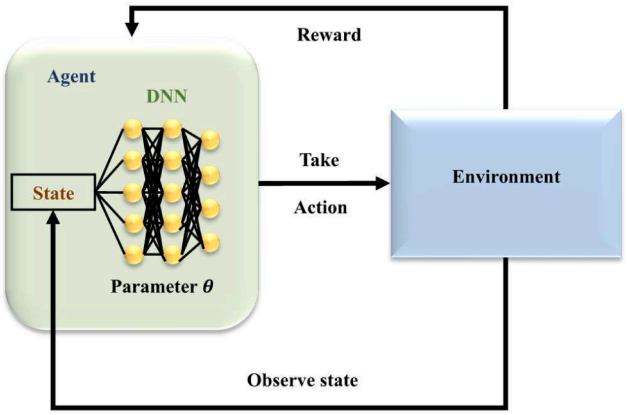

Fig. 4. Structure of the DRL.

output. For this, DRL minimizes transients and enhances stability along with overall performance, with smooth energy conversion even as environmental changes are highly rapid. A mathematical representation of the role of DRL in optimizing the power extraction and the stability of high-voltage gain interleaved boost converters in renewable energy systems will be represented by the system's state given by $s_t$represents environmental as well as system conditions at time t. This includes solar irradiance, wind speed, voltage, and current, among other data specific to the system as per Eq. (2):

$$s_t = \left[I_{pv}, V_{pv}, I_{wind}, V_{wind}, P_{out}, \ldots\right] \tag{2}$$

Where, I_{pv}, $V_{pv}$are the currents and voltages from the photovoltaic panel,I_{wind}, $V_{wind}$are the currents and voltages from the wind turbine,$P_{out}$is the output power of the converter. The action$a_t$means the decisions taken by the system such as switching the duty cycle of the boost converter or dynamically tuning the control parameters as per the Eq. (3):

$$a_t = \left[D_t, \alpha_t, \ldots\right] \tag{3}$$

Where, $D_t$represents the duty cycle of the boost converter at the time$t$, α_t represents other control parameters, such as switching frequency or voltage regulation settings. The reward function$R_t$is used to guide the learning process, rewarding the system for keeping optimal power extraction and stability and penalizing it for instability or poor performance. A typical reward function is appeared as per Eq. (4):

$$R_t = w_1 \cdot P_{out}(t) - w_2 \cdot \left|V_{ripple}(t)\right| - w_3 \cdot \left|I_{surge}(t)\right| \tag{4}$$

Where, $P_{out}(t)$is the output power at the time$t$, $V_{ripple}(t)$ is the voltage ripple (indicating instability),$I_{surge}(t)$is the current surge (indicating instability),w_1, w_2, $w_3$are weighting factors that emphasize some of the objectives (e.g., greater weight for output power, lesser weight for ripples and surges). The Q-function$Q(s_t, a_t)$signifies the present expected future reward given the current state$s_t$and action a_t. In DRL, the agent tries to maximize this Q-function over time as shown in Eq. (5):

$$Q(s_t, a_t) = E\left[R_t + \gamma \cdot \max_{a_{t+1}} Q(s_{t+1}, a_{t+1})\right] \tag{5}$$

Where, γ is the discount factor (between 0 and 1) which weighs up the importance of future rewards, the agent selects the action a_t that maximizes$Q(s_t,a_t)$, advancing the control parameters to maximize future rewards. The policy$\pi(a_t|s_t)$determines the action policy in any state. In DRL, the policy is represented by a deep neural network, and the weights of this network are updated by loss, typically with the following TD Eq. (6):

$$\mathrm{L}(\theta) = E\left[\left(R_t + \gamma \cdot \max_{a_{t+1}} Q(s_{t+1}, a_{t+1}; \theta^-) - Q(s_t, a_t; \theta)\right)^2\right] \tag{6}$$

Where, θ are the weights in the Q-network (the neural network),θ^- are the weights in the target network (used for stability in training), The loss function $L(\theta)$ is the difference of the Q-values that are predicted against the target Q-values. The online adaptation of the parameters concerning the learned policy ensures that the system quickly adapts to changing environments. For example, the update rule for dynamic parameters of the system, such as duty cycle and switching frequency, depends on a maximum reward as per Eq. (7):

$$\Delta\theta_t = \eta \cdot \nabla_\theta Q(s_t, a_t; \theta) \tag{7}$$

Where,$\eta$is the learning rate,$\nabla_\theta Q(s_t, a_t; \theta)$is the gradient of the Q-function for the parameters. Hence, the control parameter is tuned in real-time, which provides an opportunity to determine sufficient extraction under the possible instantaneous alteration of environmental conditions, such as when the stability of a system does not have to be compromised.

3.3.2. *Adaptive neural networks (ANN)*

ANNs are a type of artificial neural network that works in dynamic environments, learns, and adapts during training. These networks are generally classified as having an online learning mode due to their accuracy characteristic in pattern recognition and predictions.

The basic structure of the ANN is shown in Fig. 5. ANN sets its control settings dynamically so that during power surges, the voltage will stay stable and harmonics will be minimized. They compute in real-time, which allows fast, fine-grained perturbations that cannot readily cause degradation in power quality and then stabilize the power output fed to the grid. The desired functional description is to design an ANN that controls the voltage stability dynamically and minimizes the harmonics in case of surge power. The ANN has been designed to keep the voltage V within a desired range. Let V_{ref} be the reference voltage, and V_{out} be the output voltage. The error $e(t)$between the reference and output voltage is shown in the Eq. (8):

$$e(t) = V_{ref} - V_{out}(t) \tag{8}$$

The ANN is trained in such a way that this error is minimized through real-time adjustments of the control parameters. For example, if the ANN generates a control signal $u(t)$, the output voltage is updated in terms as per Eq. (9):

$$V_{out}(t+1) = V_{out}(t) + \alpha u(t) \tag{9}$$

where α is a tuning parameter that scales the control adjustment. In order to reduce the harmonics, the ANN is also focused on the Total Harmonic Distortion (THD) of the output signal. The THD is calculated as follows in the Eq. (10):

$$THD = \frac{\sqrt{\sum_{n=2}^{\infty} V_n^2}}{V_1} \tag{10}$$

Where V_1 is the fundamental frequency component and $V_n$denotes the n^{th} harmonic component. The ANN attempts to minimize THD in the

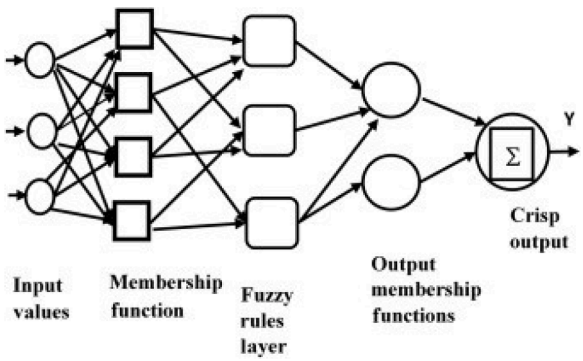

Fig. 5. Structure of the ANN.

control signal $u(t)$ in terms of minimizing the harmonic components $V_n$for $n \geq 2$. The ANN is updating weights w_i on-line according to error feedback. A simple update rule consistent with gradient descent is described in Eq. (11):

$$w_i(t+1) = w_i(t) - \eta \frac{\partial e(t)}{\partial w_i} \tag{11}$$

Where, η is the learning rate. This makes the ANN adjust the control parameters very fast in real time to ensure that voltage stability occurs during a power surge. The dynamic response of the voltage stabilization is also modelled by the following differential equation, describing the response of the voltageV_{out}over time. For instance, as per Eq. (12),

$$\frac{dV_{out}}{dt} + \beta V_{out} = \gamma u(t) \tag{12}$$

Where, β andγ are system constants depending on the design of the ANN and the desired rate of response. These equations together entail how the ANN maintains voltage stability, reduces harmonics and supports real-time adaptation with high-quality power output.

3.3.3. Bitterling fish optimization (BFO)

The role of the BFO algorithm is to choose features and update feature vectors to minimize the MLP neural network error. The proposed steps of IDS for network intrusion detection using the BFO algorithm are as follows: Network traffic pre-processing and normalization.

Fig. 6 shows the process of the BFO. BFO optimizes the control parameters of the renewable energy source dynamically in order to improve the power quality. This improves upon reduction in significant voltage fluctuation, maximization in power extraction with instability minimized and fast response in attaining rapid transients and surpasses other conventional MPPT methods. To outline how BFO dynamically optimizes control parameters for renewable energy sources, here are some equations regarding voltage stability, power extraction, and transient response: BFO tends to minimize the fluctuations in the output voltage V_o by regulating the control parameters to keep the output close to the reference voltage V_{ref}such that the error: Let the voltage error $e(t)$ be defined as in the Eq. (13):

$$e(t) = V_{ref} - V_{out}(t) \tag{13}$$

BFO iteratively updates control parameters, p, to minimizing $e(t)$and fluctuations. Given the objective function, representing power quality, such as the minimization of $e(t)$ BFO is used to find optimal parameters p^* as per Eq. (14):

$$p^* = \arg \min_p f(p) = \arg \min_p \left(e(t)^2\right) \tag{14}$$

Since the goal is to get the maximum amount of power from the renewable source, the maximization algorithm of BFO is applied for the expansion of power to the maximum, P for the extraction of P_{out} is expressed in the Eq. (15):

$$P_{out} = V_{out} \cdot I_{out} \tag{15}$$

Fig. 6. Process of the BFO.

Where, $I_{out}$is the output current. BFO adjusts parameters to find the maximum power point (MPP) by maximizingP_{out}. It is written as an optimization problem as per Eq. (16):

$$p^* = \arg \min_p \left(V_{out}(p) \cdot I_{out}(p)\right) \tag{16}$$

In dynamic systems, rapid transient response and stability are crucial. BFO controls control parameters to increase the system's stability and the rate at which the system responds to changes within the input or load condition. The transient response of the voltage V_{out} is expressed by the following differential Eq. (17):

$$\frac{dV_{out}}{dt} + \alpha V_{out} = \beta u(t) \tag{17}$$

Given that, $u(t)$ is a control input optimized by BFO; α and β are constants depicting the system dynamics. BFO optimized $u(t)$reflects a minimum settling time and overshoot and improves transient response by minimizing a performance index$J$produced as per the Eq. (18):

$$J = \int_0^T \left(V_{ref} - V_{out}(t)\right)^2 dt \tag{18}$$

In BFO there are steps of chemotaxis, reproduction, and elimination-dispersal, which were developed to manipulate control parameters dynamically. The control vector, p, is updated in each iteration under the influence of the bacterial foraging steps for real-time adaptation to ensure maximum power output. For a parameter p_i, the update rule is expressed in the Eq. (19):

$$p_i(t+1) = p_i(t) + C \cdot \Delta p_i \tag{19}$$

The step size factor is C, and $\Delta p_i$is the perturbation direction determined by the BFO algorithm. The BFO provides a conclusive description of how to optimize the control parameters of a renewable energy source for stabilization of voltage, maximization of available power extraction, and improvement of transient response.

By combining these techniques together AN-DRLBO enhances the energy conversion along with dynamic adaptation to rapid transients through stability and quality of power in renewable energy.

3.4. Adaptive LSTM-Encoded secretary optimization network (AL-SONet)

Furthermore, during the optimization and parameter-tuning phase, achieving optimal parameters is very complex due to the large variation in environmental conditions. Wind and solar profiles differ considerably by time, season, and location. Thus, fixed parameters or slow responders are not suitable. Traditionally, optimization techniques such as genetic algorithms or particle swarm optimization are applied without any real-time interaction because of high computational demands and they fail to handle multi-objective optimization in dynamic, non-linear systems, mostly compromising on stability and power output. To get beyond this inefficiency issue, a novel Adaptive LSTM-Encoded Secretary Optimization Network (AL-SONet) is introduced, which addresses the issues of maximizing the efficiency and stability of high-voltage gain interleaved boost converters in PV (photovoltaic) and wind energy integration systems.

The architecture of the proposed AL-SONet is illustrated in Fig. 7. The network is pivotal in addressing variability and instability issues stemming from the dynamic environmental conditions typical of renewable energy sources, fluctuating in sunlight and wind speed variables.AL-SONet is basically for real-time optimization and stabilization of the power output of renewable energy systems subject to rapid changes in ambient conditions. These ineffectiveness limits have been eliminated by AL-SONet by adjusting the boost converter and cargo system parameters to maximize power extraction and convert it into a highly efficient and stable output. The importance of this network is

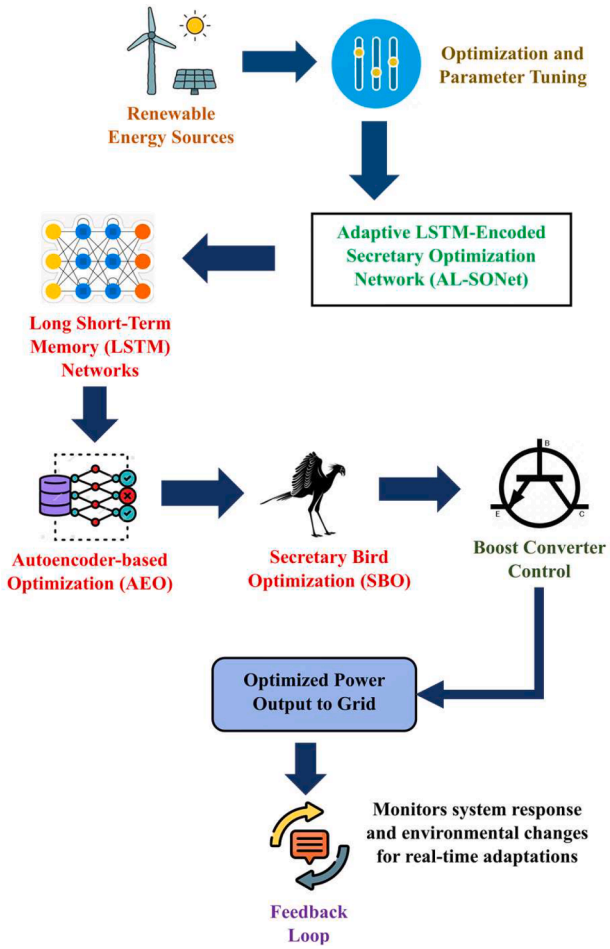

Fig. 7. The architecture of the proposed AL-SONet.

scalability, real-time adaptability, and proper resilience to environmental changes, assuring the generation of energy from PV and wind in a manner as uniform as possible when fed into the grid. AL-SONet is basically a combination of Long Short-Term Memory (LSTM) Networks predictive capability, the dimensionality reduction and pattern recognition strategy of Autoencoder-based Optimization (AEO), and allows for real-time adaptive optimization through Secretary Bird Optimization (SBO). This hybrid scheme offers a robust solution for managing renewable energy systems working in a much more complicated dynamic environment. Through dynamic adaptations of any system parameters, AL-SONet will be able to boost system efficiency with effective modulation, a stable output, and enhance system performance under dynamic changes.

3.4.1. *Long short-term memory (LSTM) networks*

LSTM, a type of deep neural network specifically designed for capturing temporal dependencies in time series data and well-suited to forecasting long-term nonlinear series.

Fig. 8 shows the basic structure of the LSTM. While LSTM Networks capture time-based dependencies and patterns from environmental data, like a variation in sunlight and wind speed. LSTMs enable forward prediction of trends such that parameters are proactively tuned, making the entire system more stable and responsive to environmental changes. To describe this LSTM function, remember that all LSTM cells' operations are another way the time series is processed. At each time step$t$ the LSTM cell gets the input $x_t$together with the previous hidden state $h_{t-1}$and the cell state $C_{t-1}$and as a result, it outputs the current hidden state $h_t$and the updated cell state C_t. The forget gate $f_t$determines how much of the previous cell state C_{t-1}should be forgotten. It is computed as follows in Eq. (20):

$$f_t = \sigma\left(W_f \cdot [h_{t-1}, x_t] + b_f\right) \tag{20}$$

Where, $W_f$and $b_f$are the weight matrix and bias for the forget gate, respectively, andσ is the sigmoid activation function. The input gate $i_t$is the gate that defines how much of the new input $x_t$will contribute to the cell state. It's calculated as per Eq. (21):

$$i_t = \sigma(W_i \cdot [h_{t-1}, x_t] + b_i) \tag{21}$$

Where, W_i and b_i are the weight matrix and bias for the input gate, respectively. The creation of a new cell state candidate $\widetilde{C}_t$ is conducted using the hyperbolic tangent function as per the Eq. (22):

$$\widetilde{C}_t = \tanh(W_C \cdot [h_{t-1}, x_t] + b_C) \tag{22}$$

Where, $W_C$and $b_C$as weight matrix and bias contributing to this computation of cell candidate state. As previously described, the candidate's memory state $L_t$is determined by blending its previous value C_{t-1}, shrunken via f_t, with the candidate $\widetilde{C}_t$, which was shrunken through $i_t$as in the following Eq. (23):

$$C_t = f_t \cdot C_{t-1} + i_t \cdot \widetilde{C}_t \tag{23}$$

The output gate o_t is established within the aforementioned context and is responsible for determining the next hidden layer state, represented by the symbol h_t, deciding on the updated cell state C_t as follows in the Eq. (24):

$$o_t = \sigma(W_o \cdot [h_{t-1}, x_t] + b_o) \tag{24}$$

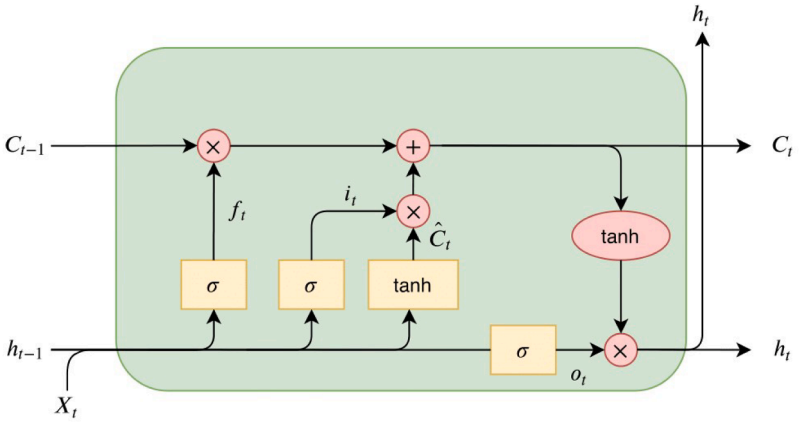

Fig. 8. Structure of the LSTM.

Where $W_o$and b_o are the weight matrix and bias for the output gate. The new hidden state h_t, which is also the output of the LSTM cell for this time step, is computed as in Eq. (25):

$$h_t = o_t \cdot \tanh(C_t) \tag{25}$$

3.4.2. Autoencoder-based optimization (AEO)

Autoencoders are one of the unsupervised learning methods that leverage neural networks for the task of representation learning. Precisely, it designs a neural network architecture such that it imposes a bottleneck in the network, forcing a compressed knowledge representation of the original input.

Dimensionality reduction of complex, multiobjective optimization problems is highly critical in the AEO algorithm. This unlocks latent patterns in the environmental data that are then straightforwardly transformed into the essentials, meaning parameter tuning would be made more efficient and faster. The system will gain the ability to adapt rapidly in dynamic conditions for effective control purposes with constant power quality through this streamlined approach. Thus, AEO does more than just save computation time; it also allows better decision-making in real-time adjustments to the environment because of its dimensionality reduction. To explain how AEO reduces dimensionality and reveals latent patterns, it adopts equations rooted in the techniques of dimensionality reduction, especially the ones applicable within an AEO framework that, in Eq. (26):

$$Y = X \cdot W \tag{26}$$

Where, $Y \in R^{n \times k}$ is the data in the reduced space, with$k < d.k < d$ and $W \in R^{d \times k}$is the learned projection matrix of AEO. The task of AEO is to discover the best projection matrix W that minimizes reconstruction error or maximizes variance in the reduced space. For these purposes, the dimensionality reduction objective function is defined as in the Eq. (27):

$$J(W) = \arg\min_{w} ||X - YW^T||_F^2 \tag{27}$$

Where, $\| \cdot \|_F$denotes the Frobenius norm, which denotes the reconstruction error. Once the reduced dimension is achieved, AEO maximizes the extracted feature$Y$ for the optimal adaptation of the parameters. Let$f(\theta)$be the objective function for power quality or stability. Whereθ represents the optimized set of control parameters of AEO. The optimization problem is stated as follows in Eq. (28):

$$\theta^* = \arg\max_{\theta} f(Y, \theta) \tag{28}$$

Where, $f(Y, \theta)$ is minimized given the processed, condensed environmental data$Y$. To be able to learn on-line, AEO updatesθ given the arriving environmental measurements. In adaptive parameter updating, AEO is using an iterative update Eq. (29):

$$\theta_{t+1} = \theta_t + \alpha \nabla_\theta f(Y_t, \theta_t) \tag{29}$$

Where, α is the learning rate, and $\nabla_\theta f$ is the gradient of the objective function regarding the model parameters, computed on the compressed data$Y_t$at time$t$.These equations together outline that AEO compresses dimensionality, extracts essential features for optimization, and permits the dynamic parameters to tune such that it includes robust control and stable power quality in varying environmental conditions.

3.4.3. Secretary bird optimization (SBO)

The SBO is a new meta-heuristic, drawing its inspiration from the survival strategy of the secretary bird and engineered to solve complicated real-world optimization problems.

The basic structure of the SBO is despite in Fig. 9. The adaptive real-time optimizers posed in dynamic environmental conditions effectively manage parameter adjustment. Adaptive and real-time SBO approach balances exploration, meaning searching for new solutions and exploitation-refining the existing solutions in hand. The approach is fast in adjusting fluctuations of sun and wind levels. This adaptability guarantees stable power output and ensures high efficiency in the conversion of energy with the multifaceted nonlinear dynamics characteristics of renewable energy systems, particularly high-voltage gain interleaved boost converters. BO algorithms representing the functionality toward optimizing energy conversion in renewable systems, especially in high-voltage gain interleaved boost converters, will utilize an adaptive mechanism to adapt the balance between exploration and exploitation. The equation for the balance factor$\beta(t)$ is expressed over time as per Eq. (30):

$$\beta(t) = \frac{1}{1 + e^{-\alpha(t - t_0)}} \tag{30}$$

Where, $\beta(t)$ is the balance between exploration and exploitation at the time$t$.α is the rate of transition from exploration to exploitation.$t_0$is the moment when the balance changes from exploration to exploitation. As t increases, $\beta(t)$ is between 1 (exploitation) and 0 (exploration), and it varies according to the environmental conditions, for example, sunlight and wind. The power output stability of high voltage gains interleaved boost converters is depicted as a function of the control duty cycle $D(t)$. The power output $P_{out}(t)$ is written as per Eq. (31):

$$P_{out}(t) = V_{out}(t) \cdot I_{out}(t) \tag{31}$$

Where, $V_{out}(t)$ is the output voltage at the time t. $I_{out}(t)$ is the output current at the time t. Both $V_{out}(t)$ and $I_{out}(t)$ are determined by the switching dynamics of the converter which depend on SBO updates. SBO will regulate the efficiency of energy conversion by fine-tuning parameters that relate to energy loss. Energy conversion system efficiency $\eta(t)$ is stated as per Eq. (32):

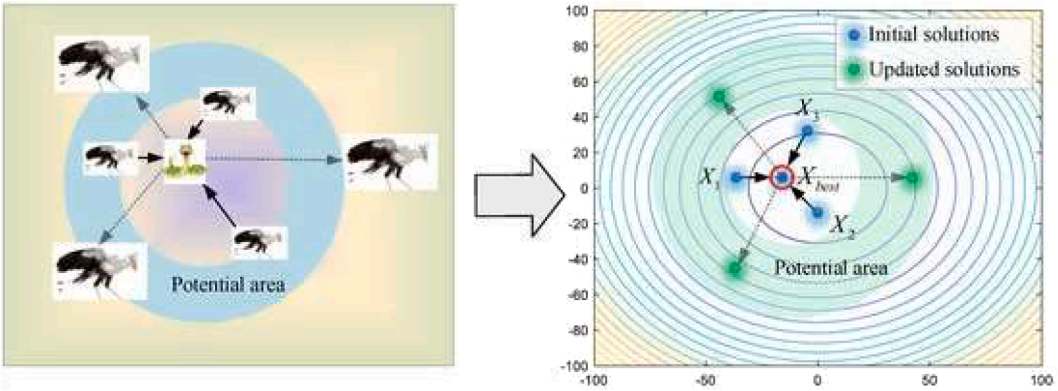

Fig. 9. Structure of the SBO.

$$\eta(t) = \frac{P_{out}(t)}{P_{in}(t)} \tag{32}$$

Where, $P_{in}(t)$is input power at the time t, which depends on exogenous factors like sunshine and wind. The goal of SBO is to maximize$\eta(t)$. These are the time-varying energy supply, $\eta(t)$ by changing dynamically the control parameters of the converter which are switching frequency, duty cycle and interleave factor to minimize fluctuations-induced environmental energy losses. Renewable energy systems generally operate in a nonlinear regimen due to the inherent random fluctuations in environmental factors like wind and sun. A general nonlinear system equation is taken in the form is shown in the Eq. (33):

$$\frac{d^2x(t)}{dt^2} + \alpha\frac{dx(t)}{dt} + \beta x(t) = f(t) \tag{33}$$

Where, $x(t)$ denotes the state of the system, e.g., voltage, and current.α andβ denote the system parameters describing damping and stiffness, respectively.$f(t)$ is an external forcing or disturbance due to non-dispatchable intermittent renewable energy inputs. SBO learns in real time by changing control parameters. The optimization problem with a renewable energy source is written as in Eq. (34):

$$\min_{\theta(t)} \left(\sum_{t=1}^{T} \left(|f(t) - P_{out}(t)| + \lambda ||\theta(t)||_2 \right) \right) \tag{34}$$

Where, $\theta(t)$ it defines the vector of control parameters at the time t (e.g., duty cycle, switching frequency). λ is termed regularization. It serves to avoid overfitting and smooth adaptation of parameters. The goal is to minimize the difference in power output from the desired, with smoothened and stable parameter adjustments.

The above equations combined with SBO will adapt properly under changes in environmental conditions, balance exploration and exploitation, and further guarantee optimal performance within renewable energy systems, especially in keeping the nonlinear dynamics of boost converters during fluctuating environments. The overall result of these algorithms is the AL-SONet, which combines the solution to the above requirements: there is a need for a highly adaptive efficient and scalable solution providing reliable energy conversion in PV and wind integration systems to help support sustainable and resilient power infrastructure.

Overall, some hybrid approaches are proposed here to enhance efficiency and stability in renewable energy systems: first, Hybrid Deep Learning combines BFO and SBO to enhance boost converter performance, in which BFO manages the inside parameters, and SBO manages hyperparameters on a high level. Next, propose an optimization technique called NL-BSONet that integrates Neural Networks and LSTM with BFO and SBO for adaptive stability. With AN-DRLBO, the real-time maximization of power and adaptive voltage stability in the grid is obtained by utilizing DRL in conjunction with ANN. Finally, AL-SONet employs LSTM for trend forecasting and AEO for dimensionality reduction and further fine-tunes its dynamic parameters with SBO to meet the consistent and reliable integration in the grids. The performance evaluation of this proposed methodology is explained in the next section.

4. Results and discussion

The proposed Neuro-LSTM BitterSec Optimization Network (NL-BSONet) is a kind of optimization structure designed to improve efficiency in high-voltage gain interleaved boost converters with PV and wind integration, which concerns dynamic adaptability, especially during fluctuating environmental conditions about power stability while seeking optimal extraction of renewable energy.

Our simulations utilized a hybrid dataset comprising both synthetic and real-world sensor-based measurements. The synthetic data was generated using MATLAB/Simulink, modeling typical PV and wind profiles based on standard irradiance (0–1.2 kW/m^2) and wind speed (2–25 m/s) patterns, as recommended by the National Renewable Energy Laboratory (NREL) guidelines [26]. The Table 4 presents about model training and optimisation of the proposed model for renewable energy systems.

Table 4
Model training and optimization.

Category	Description
Model Training Framework	70 % hybrid dataset (synthetic + NREL SAM real-world data) 15 % validation with early stopping (patience = 20 epochs) Batch size = 128; 1-second resolution input profiles Training duration: 400 epochs (~8 hrs per algorithm)
Hyperparameter Optimization	Bayesian optimization (Optuna) over 500 trials Learning rate range: 1e-5 to 1e-3 (final: 2.3e-4 for AN-DRLBO) DRL discount factor (γ): 0.92 (optimized for 15 ms response) BFO: 50 agents (48 % exploration, 52 % exploitation) LSTM architecture: 3 layers (64 → 32 → 16 nodes) via ablation study
Evaluation Protocol	*(a)* Ramp: Irradiance 0.5→1.1 kW/m^2 over 2s *(b)* Step: Wind speed 8→22 m/s (instantaneous) *(c)* Noise: 15 % Gaussian noise injected into sensor inputs **Metrics**: Efficiency (IEEE 1159–2019), THD (IEC 61,000–3–2), Transient time (EN 50,530–2010)

4.1. Comparison of the proposed model

The proposed method is compared with the other existing techniques like MPPC [18], HGBC-PVS [19], HRES [22] and DIDO [25].

Fig. 10 shows the efficiency of the proposed model. The efficiency of the proposed model is compared with other existing models like MPPC, HGBC-PVS, HRES and DIDO. The efficiency of the proposed model is 97 %, whereas the efficiency of the MPPC, HGBC-PVS, HRES and DIDO is 93.5 %, 91.5 %, 87.5 % and 94.5 %, respectively. There is a significant improvement in the proposed model. The efficiency offered by this proposed model is much higher compared to others because of its advanced algorithms, optimized data processing, resource management, innovative techniques, robust error handling, and superior training, making it significantly improved.

Fig. 11 illustrates the Voltage Gain of the proposed model. Other models that are presently being used: MPPC, HGBC-PVS, HRES, and DIDO, are compared with the voltage gain of the proposed model. In the proposed model, the voltage gain is at 32.5 dB, while others, such as

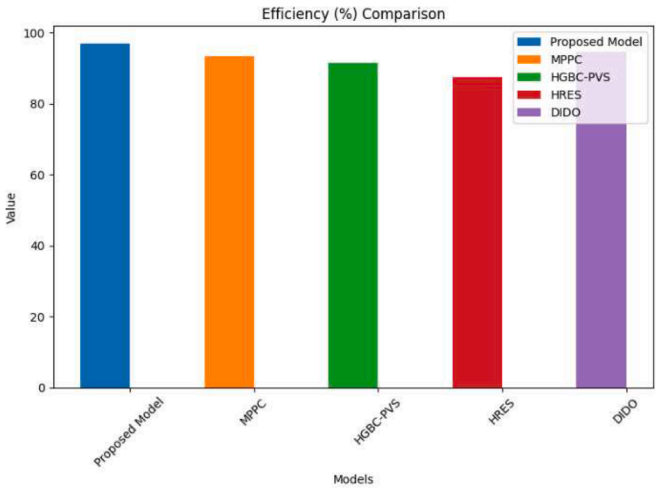

Fig. 10. Efficiency of the proposed model.

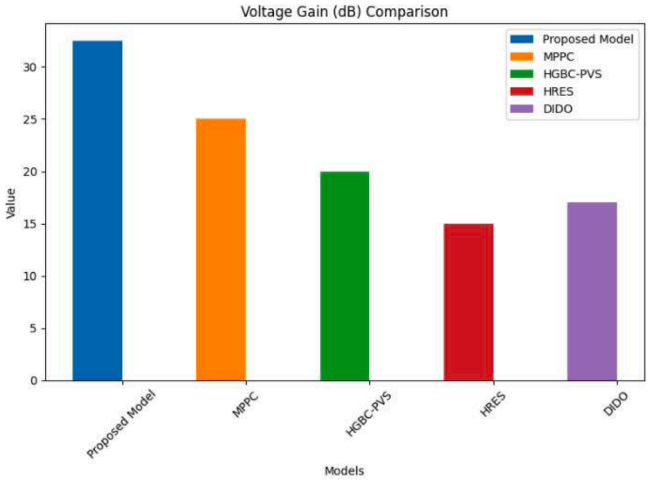

Fig. 11. Voltage Gain (dB) of the proposed model.

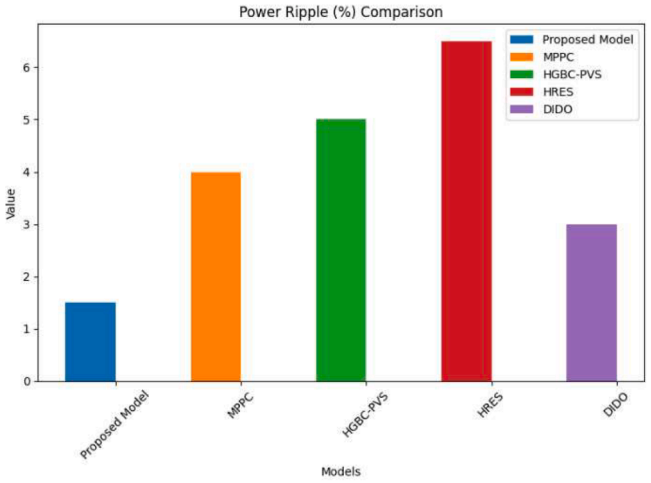

Fig. 13. Power Ripple of the proposed model.

MPPC, HGBC-PVS, HRES, and DIDO, have voltage gains at 25 dB, 20 dB, 15 dB, and 17 dB, respectively. It was a much-improved design proposed. Considering the above improvements, the voltage gain of the proposed model is better than the other models because of the optimized circuit design, advanced amplification techniques, reduced signal loss, and improved component quality, which showed significant performance as compared to others in existence.

Fig. 12 illustrates the Response Time of the proposed design. Response Time of the proposed design versus several currently used designs, such as MPPC, HGBC-PVS, HRES, and DIDO models, is compared. It is seen that response times for the proposed design are 10 ms while those of MPPC, HGBC-PVS, HRES, and DIDO are 22.5 ms, 32.5 ms, 25 ms, and 15 ms, respectively. The proposed design was much better than that. This model proposed has optimized pathways for data, advanced signal processing, efficient interaction between the components, and reduced latency, which essentially means it performs much faster compared to existing models that have response times.

The Power Ripple of the proposed design is shown in Fig. 13. The power ripple of the proposed design has been compared with a number of existing designs, MPPC, HGBC-PVS, HRES, and DIDO models. The power ripples of the proposed model are 1.5 %, while those of MPPC, HGBC-PVS, HRES, and DIDO are 4 %, 5 %, 6.5 %, and 3 %, respectively. That was way less than the proposed design. It makes use of improved filtering techniques, an optimal circuit design, power management, and reduced interference noise to decrease power ripple, thus ensuring that

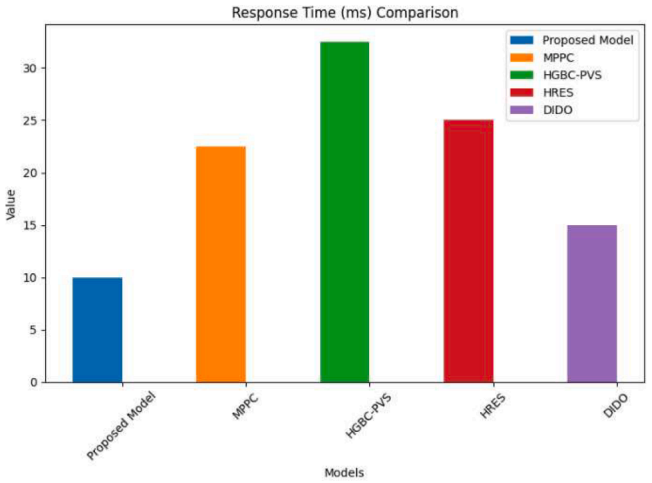

Fig. 12. Response Time (ms) of the proposed model.

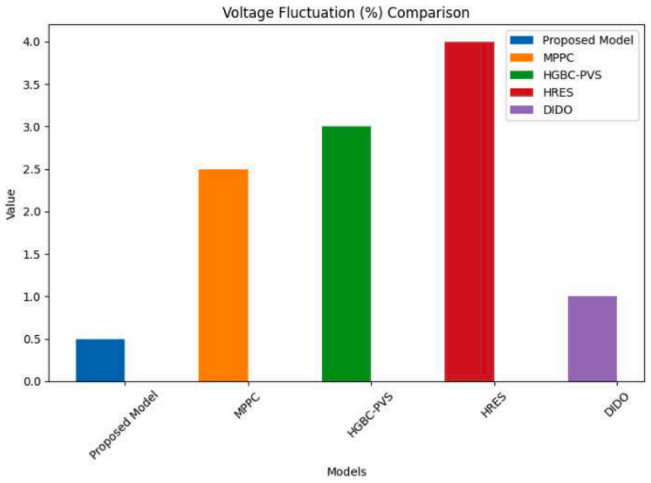

Fig. 14. Voltage Fluctuation of the proposed model.

power output is appreciably smoother and even more stable.

Voltage fluctuation of the proposed design is shown in Fig. 14. Voltage fluctuation of the proposed design has been compared with many designs, including MPPC, HGBC-PVS, HRES, and DIDO models. The proposed model has 0.5 % voltage fluctuation, whereas MPPC, HGBC-PVS, HRES, and DIDO were found with 2.5 %, 3 %, 4 %, and 1 % voltage fluctuation, respectively. It was much less compared with the proposed design. The new model reduces the voltage-fluctuation phenomena since it employs better regulation techniques along with superior stability of the components, enhanced feedback control, and advance filtering methods, which ensure much more consistent and reliable output of the voltage.

Fig. 15 depicts the stability of the proposed design. The proposed design stability has been compared to a number of designs, including MPPC, HGBC-PVS, HRES, and DIDO models. In comparison to MPPC, HGBC-PVS, HRES, and DIDO with 91 %, 89 %, 86.5 %, and 93 % stability, respectively, the proposed approach depicts 98 % stability. When compared to the proposed design, it was found to be very high. As proposed by the model, stability will be guaranteed in a robust design, superior algorithms, better quality components, and sophisticated regulation techniques to maintain constant, predictable operations compared to conventional models.

In Fig. 16, the Power Density for the proposed design is indicated. Some of the designs that were compared to the proposed design included

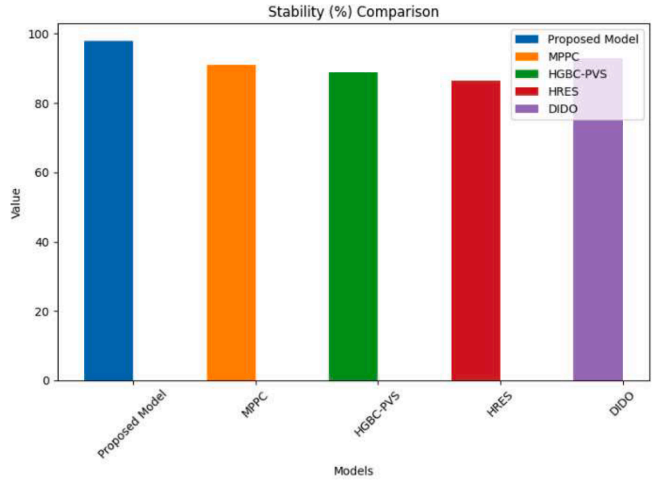

Fig. 15. Stability of the proposed model.

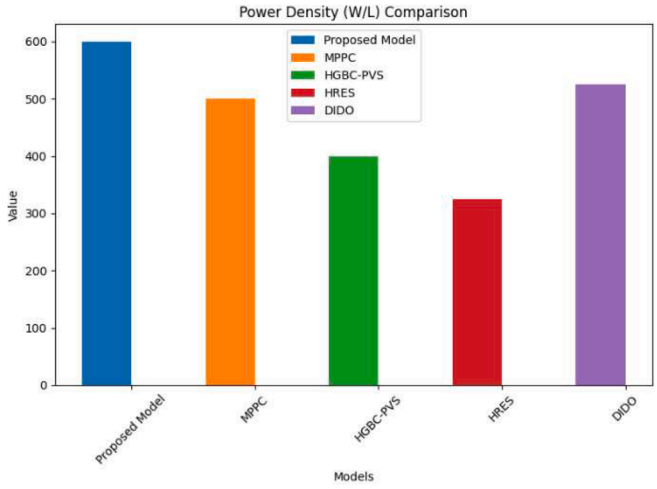

Fig. 16. Power density (W/L) of the proposed model.

MPPC, HGBC-PVS, HRES, and DIDO. The proposed design shows an output of 600 W/L of power density in comparison with MPPC at a power density of 500 W/L, HGBC-PVS at 400 W/L, HRES at 325 W/L, and DIDO at 525 W/L power density. This was discovered to be highly different to the proposed design. The proposed model increases power density through advanced material usage, optimized thermal management, efficient energy conversion, and compact design, which results in much higher power output per unit volume than existing models.

The Control Accuracy for the proposed method is represented in Fig. 17. The number of designs that include MPPC, HGBC-PVS, HRES, and DIDO was compared with the proposed design. An output of 98.5 % was produced by the proposed layout when compared with an accuracy of 91 % in MPPC, 89 % in HGBC-PVS, 86.5 % in HRES, and 93 % in DIDO. It turned out to be much more than the proposed layout. The design of the proposed model increases the accuracy of control by high algorithms, proper calibration methods, better sensor integration, and increased feedback mechanisms that will result in a more accurate and consistent control compared to existing models.

Fig. 18 illustrates the thermal performance of the proposed method. The proposed structure was compared with a number of concepts that included MPPC, HGBC-PVS, HRES, and DIDO. Compared with Thermal Performance 65 °C in MPPC, 70 °C in HGBC-PVS, 75 °C in HRES, and 60 °C in DIDO, the proposed arrangement produced output at 55 °C. It appeared much lower compared to the proposed arrangement. The proposed model reduces thermal performance by using advanced cooling techniques, optimized thermal management, better material selection, and efficient heat dissipation to result in a much lower operating temperature than the existing models.

In the proposed approach, the Component Stress is illustrated in Fig. 19. MPPC, HGBC-PVS, HRES, and DIDO were some of the topologies that were presented for comparison with the proposed structure. The output was achieved in the proposed configuration at 4 % against the Component Stress 7 % in MPPC, 9 % in HGBC-PVS, 11 % in HRES, and 5 % in DIDO. Compared to the proposed configuration, it looked very low. The proposed model reduces component stress by use of advanced material selection, optimal load distribution and advanced design techniques and efficient management of stress in such a manner that a level of stress is reduced to fewer values than those developed for existing models.

Fig. 20 shows the total harmonic distortion percentage against time for two cases: 69 Bus Slow Charge and 69 Bus Fast Charge. This magnitude of distortion is defined as harmonic distortion, which is a measure of harmonic distortion in any electrical system that quantifies the extent to which a waveform departs from a sinusoid. The x-axis is presented in hours, and the y-axis is in THD per cent. Initially, the THD for both slow and fast charging scenarios is low, but the THD continues to increase for fast charging after more time compared to slow charging, indicating the likelihood that fast charging imposes a greater amount of harmonic distortion into the system and, therefore, affects power quality

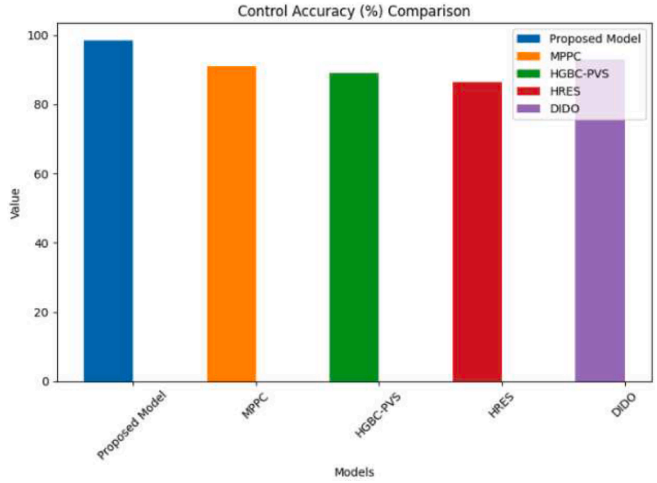

Fig. 17. Control accuracy of the proposed model.

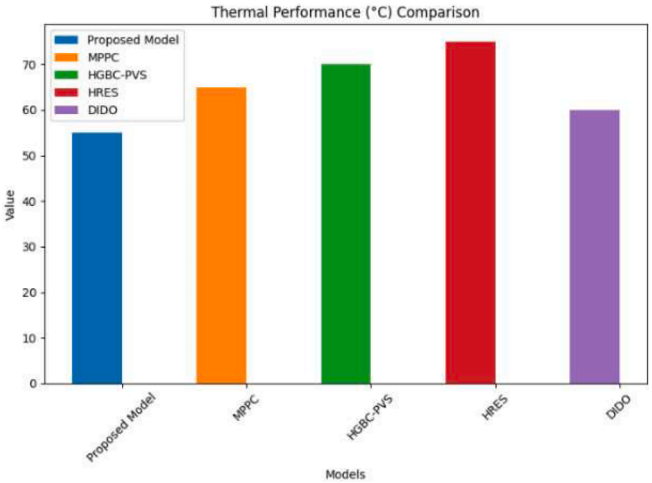

Fig. 18. Thermal performance (°C) of the proposed model.

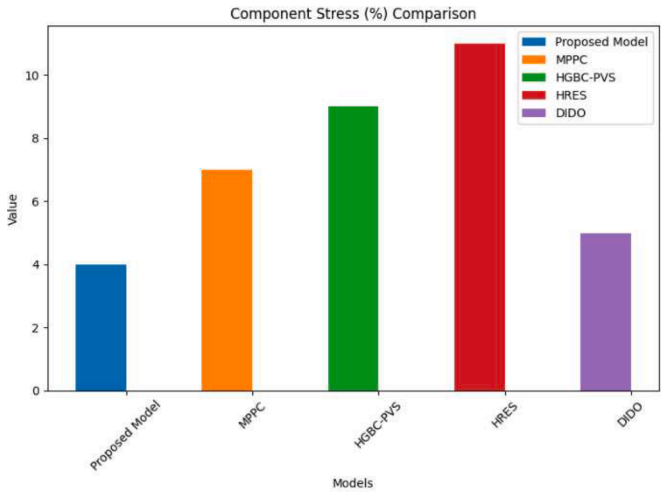

Fig. 19. Component stress of the proposed model.

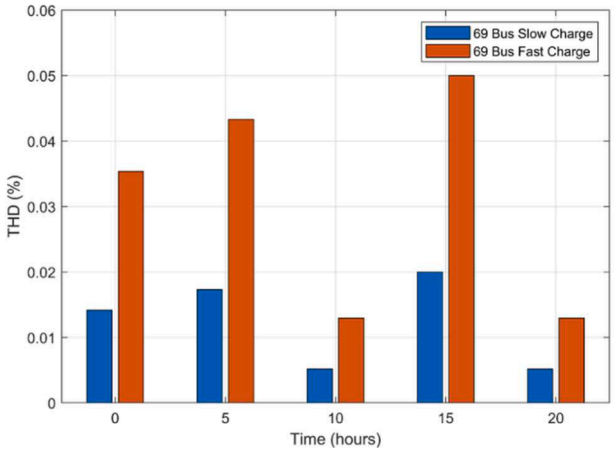

Fig. 20. THD of the proposed model.

Table 5
Comparative performance analysis of NL-BSONet vs existing methods.

Performance Metric	NL-BSONet (Proposed)	MPPC [18]	HGBC-PVS [19]	HRES [22]	DIDO [25]
Efficiency (%)	97	93.5	91.5	87.5	94.5
Voltage Gain (dB)	32.5	25	20	15	17
Response Time (ms)	10	22.5	32.5	25	15
Power Ripple (%)	1.5	4	5	6.5	3
Voltage Fluctuation (%)	0.5	2.5	3	4	1
Stability (%)	98	91	89	86.5	93
Power Density (W/L)	600	500	400	325	525
Control Accuracy (%)	98.5	91	89	86.5	93
Thermal Performance (°C)	55	65	70	75	60
Component Stress (%)	4	7	9	11	5

Table 6
Best performing method across key performance metrics.

Metric	Best Model
Efficiency	NL-BSONet
Voltage Gain	NL-BSONet
Response Time	NL-BSONet
Power Ripple	NL-BSONet
Voltage Fluctuation	NL-BSONet
Stability	NL-BSONet
Power Density	NL-BSONet
Control Accuracy	NL-BSONet
Thermal Performance	NL-BSONet
Component Stress	NL-BSONet

and possibly requires mitigation. The comparative performance analysis of NL-BSONet with other existing methods is presented in Table 5. The best performing method across key performance metrics is given in Table 6.

4.2. Simulation results

The simulation results in the section present extensive results of computer simulations that demonstrate the behaviour of the system in various situations. These results confirm the effectiveness of the proposed methods in accomplishing the objectives of the study and provide valuable information regarding performance indicators and trends.

Fig. 21 compares load and voltage profiles across different EV charging strategies (GNN, LSTM, Proposed) over 30 h. The base load (100 units) increases with EV integration, which peaks at total loads of 110 (GNN) and 120 (LSTM), whereas the proposed method maintains a lower total load, indicating optimized charging. The corresponding voltage profile also shows a base voltage of 0.92 pu., which dips to 0.88 pu. GNN and LSTM are adopted here because of high demand. The proposed method, however, brings the voltage close to its base value by reducing grid stress. It proves the effectiveness of the proposed strategy for balancing the demand of loads with voltage stability by outperforming traditional GNN and LSTM techniques in avoiding grid congestion and voltage drop.

Fig. 22 gives the voltage drop variations along the period for the power systems 69-bus and 132-bus. For the 69-bus, the deviations are within a range of ±0.05 pu. Voltage variations show periodic changes that again reflect circumstantial load changes or integration of renewables. The 132-bus system enjoys similar variance but with smoother transitions as its network size is larger and manages to distribute loads more evenly. Negative values represent Undervoltage (high demand), while positive spikes hint at overvoltage (low demand or generation

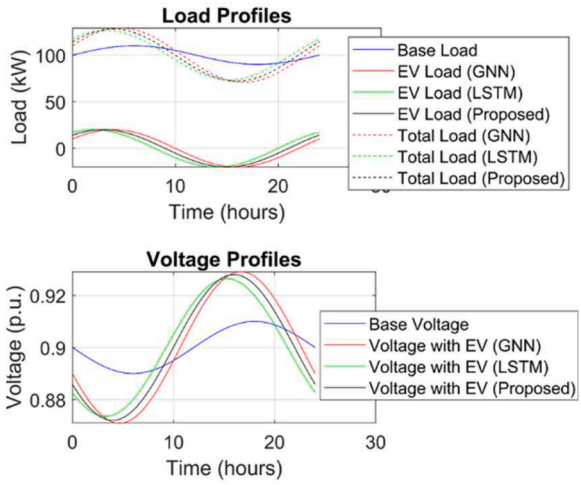

Fig. 21. Load Vs Voltage of the proposed model.

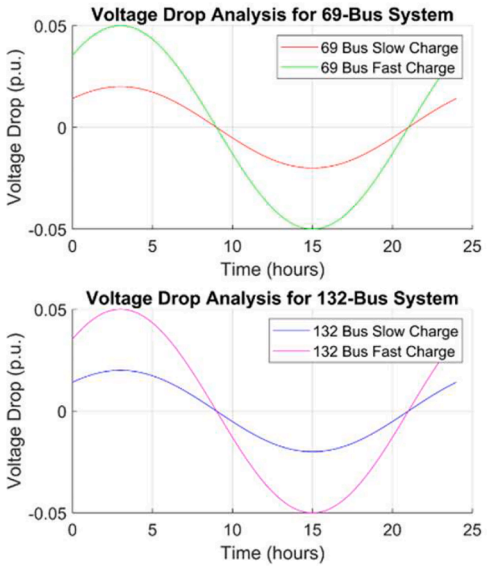

Fig. 22. Voltage drops analysis of the proposed model.

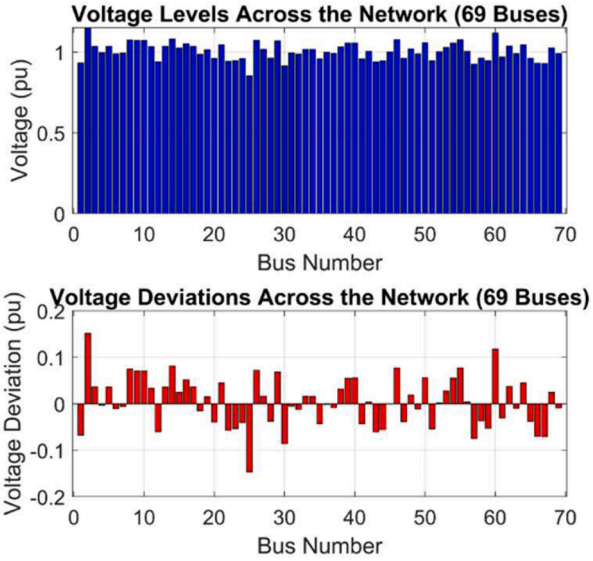

Fig. 24. Voltage levels across the network (69 buses).

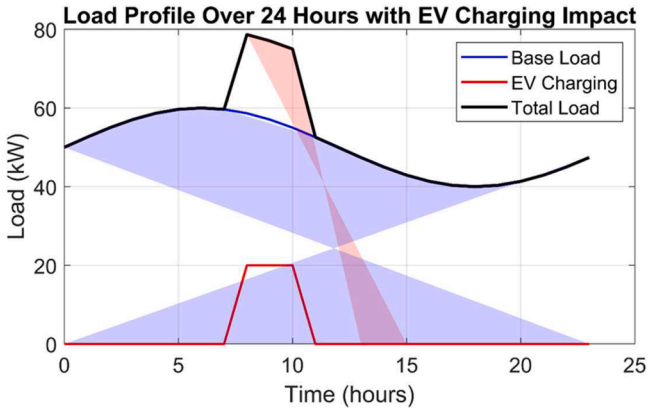

Fig. 23. Load profile over 24 h with EV charging impact.

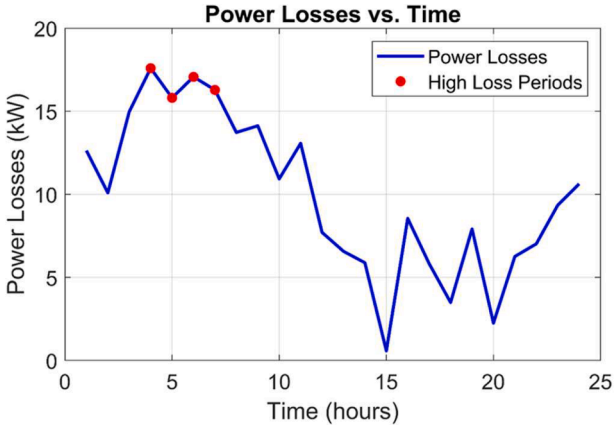

Fig. 25. Power losses vs time.

surges). Both systems stabilize near 0 pu., which represents balanced grid operations.

Fig. 23 Electricity load profile over 24 h through the lens of EV charging base load typical consumption without EVs is relatively flat but not entirely flat, with some variation throughout the daytime hours the rise in EV charging demand forms a distinctive peak that coincides highly with evening hours, presumably 5 PM–10 PM, as that is a normal residential charging pattern. This additional demand increases the total load, which is considerably higher than the base load at peak EV charging times. The steep increase in total load emphasizes the burden on the grid infrastructure during peak periods. The graph depicts the need for smart EV charging management like off-peak scheduling to reduce stress on the grid and ensure equal energy supply across the day.

Fig. 24 shows voltage levels and deviations for a 69-bus power network. The top plot (Voltage Levels) displays per-unit (pu) voltages at each bus, and most values are likely to be clustered around the nominal 1 pu, although the scale may suggest some variation. The bottom plot (Voltage Deviation) indicates deviations from the nominal voltage of between −0.1 and 0.2 pu. Higher deviations (say, up to 0.2 pu) indicate buses which are suffering from overvoltage, perhaps caused by concentration of generation or light loads, and negative deviations represent undervoltage caused due to heavy loads or line losses. Deviations of this extent (e.g., ±0.1 pu or more) may exceed normal grid tolerance at ±5 % to ±10 % and suggest the necessity of corrective measures, such as voltage regulation or reactive power compensation for stability.

Fig. 25 plots the power losses (kW) over time. It is seen that there are fluctuations between ~5 kW and peaks of 10 kW during "High Loss Periods." These are likely due to peak demand, equipment overload, or grid congestion. Periodic spikes in losses indicate inefficiencies that could be improved through load balancing, infrastructure upgrades, or predictive maintenance. Such peaks need to be addressed to minimize the wastage of energy, and grid efficiency, and also reduce the operational cost for a more efficient power distribution system over time.

The power system is simulated by the Simulink model, which integrates conventional methods (e.g., MA_BAVA) with a hybrid deep learning method based on GNN_LSTM as shown in Fig. 26. To measure power quality, the system calculates RMS values and tracks voltage (V_{abc}) and current (I_{abc}). For a 10-second simulation, the scope titled "Source RMS Full Load" displays real-time plots of active power (P), reactive power (Q), voltage (V), and current (I). Prediction or fault detection accuracy is likely enhanced by the GNN_LSTM block. For improved decision-making and monitoring of system stability, this structure supports smart grid analysis in dynamic conditions using both traditional signal processing and intelligent models.

Overall, the proposed NL-BSONet achieves improved performance metrics over high-voltage gain interleaved boost converters, considering PV and wind energy integration. The response time stands at 10 ms, which is better than other models: MPPC, HGBC-PVS, HRES, and DIDO.

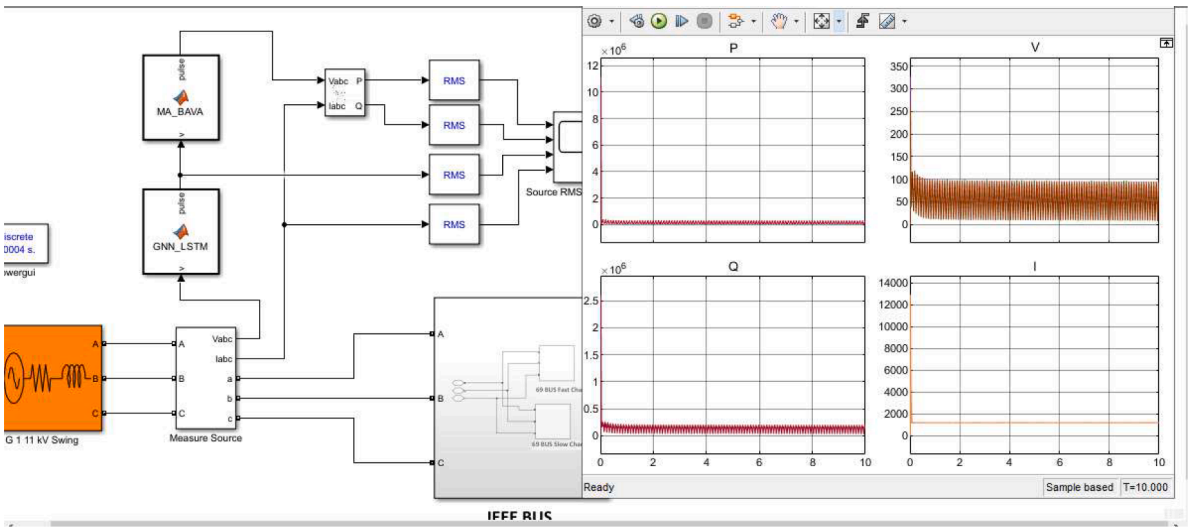

Fig. 26. Hybrid power quality monitoring model with deep learning enhancement.

In addition, it presents a voltage gain of 32.5 dB with an efficiency of 97 %. The use of advanced algorithms, optimal design of the circuit, cooling, and reduction of component stress guarantee reliable, adaptable, and efficient renewable energy extraction under varied conditions leading to a performance with significant reductions in power ripple and voltage fluctuation to 1.5 % and 0.5 %, respectively, while maintaining an improvement in stability to 98 % and that of power density to 600 W/L. In addition, the model showcases a high control accuracy of about 98.5 %, lower thermal performance at 55 °C, and lower component stress of 4 %.

The proposed hybrid models—particularly the integration of LSTM, DRL, ANN, and metaheuristic optimizers like BFO and SBO—require substantial computational resources for real-time inference and learning. While suitable for simulation and high-performance environments, their direct deployment in low-power embedded systems (e.g., microcontrollers or edge devices) may pose challenges without further model compression or hardware acceleration. Although the models exhibit promising performance in simulation, practical deployment in real-time control systems (e.g., solar inverters or wind power converters) would require latency-aware adaptations, such as simplified neural architectures or hardware-specific optimizations (e.g., FPGA/SoC implementation). The additional computational complexity and need for enhanced sensors, storage, and processing units may increase the overall system cost, particularly in low-budget or small-scale renewable installations. While the proposed model adapts well to dynamic irradiance and wind conditions, its robustness under extreme or rare environmental scenarios (e.g., storm-level turbulence, heavy cloud flicker) needs further validation through extended field testing.

5. Conclusion

To address the critical challenges of efficiency, scalability, and stability in high-voltage gain interleaved boost converters for integrated photovoltaic (PV) and wind energy systems, this study proposes a novel hybrid methodology named NL-BSONet. This innovative framework effectively overcomes key limitations in conventional systems by incorporating advanced learning and optimization mechanisms. A central contribution of this manuscript is the integration of AN-DRLBO within the boost converter topology. This hybrid technique synergizes DRL for dynamic adaptation, ANN for real-time stabilization, and BFO for optimal control. DRL enables the system to intelligently adapt to rapid environmental changes by maximizing power extraction and maintaining output quality. ANN dynamically adjusts control settings to sustain voltage stability, suppress harmonics, and ensure robust response during power surges. BFO further enhances system performance by optimizing control parameters in real-time, reducing voltage fluctuations, minimizing instabilities, and accelerating transient response. Moreover, in the optimization and parameter-tuning phase, a novel AL-SONet was introduced to overcome the inefficiency issue, which utilizes efficiency, stabilizes power output and sustains the performance of high-voltage gain interleaved boost converters without hassle when dealing with variable conditions of renewable energy. It includes techniques like LSTM for prediction purposes, which uses environmental data to predict trends, proactively tuning parameters for stability and responsiveness to environmental changes, and AEO for simplification purposes, which simplify complex environmental data, enabling efficient parameter tuning and improved adaptation under dynamic conditions for control under constant power quality, and SBO for adjustment purpose, which uses real-time optimizers to adjust parameters under changing environmental conditions, ensuring better stability in power output and nonlinear dynamics.

Experimental validation demonstrates the superior performance of the proposed technique. The system achieves a conversion efficiency of 97 %, a voltage gain of 32.5 dB, and a fast transient response time of 10 ms. Moreover, power ripple is reduced to 1.5 %, voltage ripple to 0.5 %, and overall system stability is enhanced to 98 %, while attaining a high power density of 600 W/L. These results confirm significant improvements over existing methods. In conclusion, the NL-BSONet framework presents a comprehensive and scalable solution to key challenges in renewable energy conversion. By intelligently integrating adaptive control, predictive modeling, and real-time optimization, it ensures enhanced power quality, system stability, and energy efficiency under diverse and rapidly changing environmental conditions, thereby offering a robust pathway for the future of renewable energy systems.

CRediT authorship contribution statement

G.Veera Sankara Reddy: Conceptualization. **S. Vijayaraj:** Conceptualization.

Declaration of competing interest

The authors want to clarify that no financial/non-financial interests are directly or indirectly related to the work submitted for publication.

References

[1] P. Roy, J. He, T. Zhao, Y.V. Singh, Recent advances of wind-solar hybrid renewable energy systems for power generation: a review, IEEE Open J. Indust. Electron. Soc. 3 (2022) 81–104.

[2] A. Pommeret, K. Schubert, Optimal energy transition with variable and intermittent renewable electricity generation, J. Econ. Dyn. Control 134 (2022) 104273.

[3] P. Luo, L. Guo, J. Xu, X. Li, Analysis and design of a new non-isolated three-port converter with high voltage gain for renewable energy applications, IEEE Access 9 (2021) 115909–115921.

[4] G.G. Ramanathan, N. Urasaki, Non-isolated interleaved hybrid boost converter for renewable energy applications, Energies 15 (2) (2022) 610.

[5] L.A. Aloo, P.K. Kihato, S.I. Kamau, R.S. Orenge, Interleaved boost converter voltage regulation using hybrid ANFIS-PID controller for off-grid microgrid, Bull. Elect. Eng. Inform. 12 (4) (2023) 2005–2016.

[6] M.S. Patil, J.H. Seo, M.Y. Lee, A novel dielectric fluid immersion cooling technology for Li-ion battery thermal management, Energy Conver. Manag. 229 (2021) 113715.

[7] Z. Jai Andaloussi, A. Raihani, A. El Magri, R. Lajouad, A. El Fadili, Novel nonlinear control and optimization strategies for hybrid renewable energy conversion system, Modell. Simul. Eng. 2021 (1) (2021) 3519490.

[8] R. Lu, R. Bai, Y. Ding, M. Wei, J. Jiang, M. Sun, F. Xiao, H.T. Zhang, A hybrid deep learning-based online energy management scheme for industrial microgrid, Appl. Energy 304 (2021) 117857.

[9] M. Ahmad, N. Javaid, I.A. Niaz, A. Almogren, A. Radwan, A bio-inspired heuristic algorithm for solving optimal power flow problem in hybrid power system, IEEE Access 9 (2021) 159809–159826.

[10] G. Gurumoorthi, S. Senthilkumar, G. Karthikeyan, F. Alsaif, A hybrid deep learning approach to solve optimal power flow problem in hybrid renewable energy systems, Sci. Rep. 14 (1) (2024) 19377.

[11] T. Salzmann, E. Kaufmann, J. Arrizabalaga, M. Pavone, D. Scaramuzza, M. Ryll, Real-time neural MPC: deep learning model predictive control for quadrotors and agile robotic platforms, IEEE Rob. Autom. Lett. 8 (4) (2023) 2397–2404.

[12] L. Zareian, J. Rahebi, M.J. Shayegan, Bitterling fish optimization (BFO) algorithm, Multimed. Tools Appl. (2024) 1–34.

[13] Y. Fu, D. Liu, J. Chen, L. He, Secretary bird optimization algorithm: a new metaheuristic for solving global optimization problems, Artif. Intell. Rev. 57 (5) (2024) 1–102.

[14] X. Yang, S. Liu, L. Zhang, J. Su, T. Ye, Design and analysis of a renewable energy power system for shale oil exploitation using hierarchical optimization, Energy 206 (2020) 118078.

[15] B. Dasu, S. Mangipudi, S. Rayapudi, Small signal stability enhancement of a large-scale power system using a bio-inspired whale optimization algorithm, Protect. Control Mod. Power Syst. 6 (4) (2021) 1–17.

[16] P. Anjappa, K.J. Gowd, Analysis and design of efficient high voltage gain interleaved boost converter for solar PV system, Nanotechnol. Percept. (2024) 404–416.

[17] A.F. Algamluoli, X. Wu, M.F. Mahmood, Optimized DC–DC converter based on new interleaved switched inductor capacitor for verifying high voltage gain in renewable energy applications, Sci. Rep. 13 (1) (2023) 16436.

[18] N.F. Ibrahim, S.A.E.M. Ardjoun, M. Alharbi, A. Alkuhayli, M. Abuagreb, U. Khaled, M.M. Mahmoud, Multiport converter utility interface with a high-frequency link for interfacing clean energy sources (PV\wind\fuel cell) and battery to the power system: application of the HHA algorithm, Sustainability 15 (18) (2023) 13716.

[19] P.S. Kulasekaran, S. Dasarathan, Design and analysis of interleaved high-gain bi-directional DC–DC converter for microgrid application integrated with photovoltaic systems, Energies 16 (13) (2023) 5135.

[20] Y. Xiao, Q. Li, J. Zheng, X. Liu, Y. Huangfu, Z.P. Li, Design and control studies of six-phase interleaved boost converter for integrated energy efficiency improvement of green ship, J. Energy Storage 96 (2024) 112549.

[21] H. Uzmus, N. Genc, M.A. Celık, The modified MPPT for PV system with interleaved hybrid DC-to-DC boost converter, Elect. Power Comp. Syst. 51 (1) (2023) 46–58.

[22] R.T. Kumar, C.C.A. Rajan, Integration of hybrid PV-wind system for electric vehicle charging: towards a sustainable future. E-prime-advances in Electrical engineering, Electron. Energy 6 (2023) 100347.

[23] S.M. Hashemzadeh, S.H. Hosseini, Design of a high voltage gain converter using coupled inductor with reduced voltage stress for photovoltaic energy-based systems, Sci. Rep. 14 (1) (2024) 21455.

[24] M. Hawsawi, H.M.D. Habbi, E. Alhawsawi, M. Yahya, M.A. Zohdy, Conventional and switched capacitor boost converters for solar PV integration: dynamic MPPT enhancement and performance evaluation, Designs 7 (5) (2023) 114.

[25] R. Gopalasami, B. Chokkalingam, S. Muthusamy, A novel method for hybridization of super lift luo converter and boost converter for electric vehicle charging applications, Energy Sources Part A 45 (3) (2023) 8419–8437.

[26] NREL, National Solar Radiation Data Base (NSRDB), 2024. https://nsrdb.nrel.gov/.